LAWRENCE
LIVERMORE
NATIONAL
LABORATORY

LLNL-TR-599052

NOx Sensor Development

L. Y. Woo, R. S. Glass

November 6, 2012

Disclaimer

This work performed under the auspices of the U.S. Department of Energy by Lawrence Livermore National Laboratory under Contract DE-AC52-07NA27344.

Project 18518 – Materials for High Efficiency Engines

Agreement 8697 - NO_x Sensor Development

Leta Y. Woo and Robert S. Glass
Lawrence Livermore National Laboratory
P.O. Box 808, L-103
Livermore, CA 94551-9900
(925) 423-7140; fax: (925) (422-5844); e-mail: glass3@llnl.gov

DOE Technology Manager: Jerry L. Gibbs
(202) 586-1182; fax: (202) 586-1600; e-mail: jerry.gibbs@ee.doe.gov

Contractor: Lawrence Livermore National Laboratory, Livermore, California
Prime Contract No.: W-7405-Eng-48; LLNL-TR-510234

Objectives

- Develop an inexpensive, rapid-response, high-sensitivity and selective electrochemical sensor for oxides of nitrogen (NO_x) for compression-ignition, direct-injection (CIDI) OBD II systems
- Explore and characterize novel, effective sensing methodologies based on impedance measurements and designs and manufacturing methods that are compatible with mass fabrication
- Transfer the technology to industry for commercialization

Approach

- Use an ionic (O^{2-}) conducting ceramic as a solid electrolyte and metal or metal-oxide electrodes
- Correlate NO_x concentration with changes in cell impedance
- Evaluate sensing mechanisms and aging effects on long-term performance using electrochemical techniques
- Collaborate with Ford Research Center and EmiSense Technologies, LLC to optimize sensor performance and perform dynamometer and on-vehicle testing

Accomplishments

- Developed a Cooperative Research and Development Agreement (CRADA) with EmiSense Technologies, LLC, a Salt Lake City, UT company which has licensed the LLNL NO_x sensor technology
- Completed advanced engine dynamometer testing at Ford Motor Company of FY12 prototypes demonstrating robust performance under aggressive driving conditions
- Publications/Presentations:
    - W. L. Du Frane, L.Y. Woo, R.S. Glass, R.F. Novak, and J.H. Visser, "Substrate Effects on Electrochemical NO_x Sensor Based on Porous Y_2O_3-Stabilized ZrO_2 (YSZ) and Sr-doped $LaMnO_3$ (LSM), presented at the 221st Meeting of the Electrochemical Society, Seattle, Washington, May 6-10, 2012.
    - W. L. Du Frane, L.Y. Woo, R.S. Glass, R.F. Novak, and J.H. Visser, "Substrate Effects on Electrochemical NO_x Sensor Based on Porous Y_2O_3-Stabilized ZrO_2 (YSZ) and Sr-doped $LaMnO_3$ (LSM). *ECS Transactions*, submitted 2012.
    - L.Y.Woo and R. S. Glass, "NO_x Sensor Development," project ID #PM005, Annual Merit Review and Peer Evaluation. Washington, D.C., May 15, 2012

Future Directions

- Finish the development of more advanced prototypes suitable for cost-effective, mass manufacturing and for optimizing performance, including long-term stability and cross-sensitivity, in laboratory, dynamometer, and on-vehicle tests
- Working through the CRADA with EmiSense Technologies, LLC, and in collaboration with Ford Motor Company, bring the NO_x sensor technology to commercialization

Introduction

NO_x compounds, specifically NO and NO_2, are pollutants and potent greenhouse gases. Compact and inexpensive NO_x sensors are necessary in the next generation of diesel (CIDI) automobiles to meet government emission requirements and enable the more rapid introduction of more efficient, higher fuel economy CIDI vehicles.[1-3]

Because the need for a NO_x sensor is recent and the performance requirements are extremely challenging, most are still in the development phase.[4-6] Currently, there is only one type of NO_x sensor that is sold commercially, and it seems unlikely to be able to meet more stringent future emission requirements.

Automotive exhaust sensor development has focused on solid-state electrochemical technology, which has proven to be robust for in-situ operation in harsh, high-temperature environments (e.g., the oxygen stoichiometric sensor). Solid-state sensors typically rely on yttria-stabilized zirconia (YSZ) as the oxygen-ion conducting electrolyte, which has been extensively explored, and then target different types of metal or metal-oxide electrodes to optimize the response.[2-6]

Electrochemical sensors can be operated in different modes, including amperometric (current based) and potentiometric (potential based), both of which are direct current (dc) measurements. Amperometric operation is costly due to the electronics necessary to measure the small sensor signal (nanoampere current at ppm NO_x levels), and cannot be easily improved to meet the future technical performance requirements. Potentiometric operation has not demonstrated enough promise in meeting long-term stability requirements, where the voltage signal drift is thought to be due to aging effects associated with electrically driven changes, both morphological and compositional, in the sensor.[7]

Our approach involves impedancemetric operation, which uses alternating current (ac) measurements at a specified frequency. The approach is described in detail in previous reports and several publications.[8-12] Impedancemetric operation has shown the potential to overcome the drawbacks of other approaches, including higher sensitivity towards NO_x, better long-term stability, potential for subtracting out background interferences, total NO_x measurement, and lower cost materials and operation.[8-11]

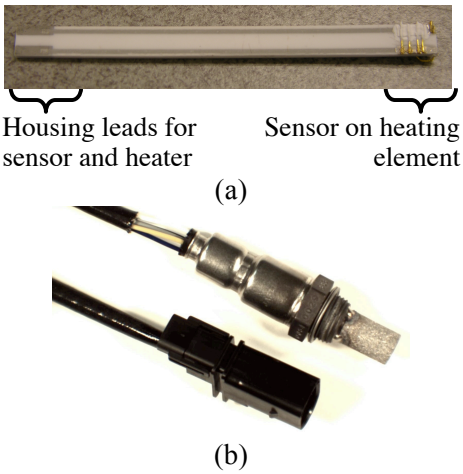

Figure 1. Picture of (a) alumina substrate with imbedded heater, provided by Ford Motor Company, suitable for packaging into (b) protective sensor housing.

Past LLNL research and development efforts have focused on characterizing different sensor materials and understanding complex sensing mechanisms.[8-12] Continued effort has led to improved prototypes with better performance, including increased sensitivity (to less than 5 ppm) and long-term stability, with more appropriate designs for mass fabrication, including incorporation of an alumina substrate with an imbedded heater and a protective sensor housing (see Fig. 1). Using multiple frequency measurements, an algorithm has been developed to subtract out that portion of the response due to interfering species.

Efforts in FY2012 have continued building on previous work to modify prototypes to improve per-

formance, including drift and sample-to-sample reproducibility. Other progress this year includes dynamometer testing using advanced emission test protocols to confirm robustness and durability in FY12 prototypes. As noted above, the LLNL NO_x sensor technology has been licensed to EmiSense Technologies, located in Salt Lake City, and another accomplishment this past year was the development of a CRADA for joint development activities. This will greatly accelerate the commercialization efforts for this technology.

Background

For a two-electrode electrochemical cell, impedancemetric sensing requires that at least one of the electrodes act as the "sensing" electrode with selective response to NO_x over other gas phase components. This contrasts to the case in potentiometric sensing, which relies on differential measurements between the two electrodes. The impedancemetric sensor design is quite flexible and can either contain one sensing electrode and one counter (i.e., non-sensing) electrode, or two sensing electrodes. It opens up the opportunity to use a wide variety of materials, both metal and metal oxides.

Both electrode composition and microstructure influence sensitivity, which relies on limiting the oxygen reaction on the electrode so that the NO_x reaction can be resolved.[9-11] In general, for the "sensing" electrode a dense microstructure is required with appropriate composition to limit the catalytic activity towards oxygen.[10-11]

Measured sensor impedance is a complex quantity with both magnitude and phase angle information. The phase angle has been found to provide a more stable response at higher operating frequencies and we prefer it for the sensor signal.[8-12]

In previous work, impedancemetric sensing using either gold or strontium-doped lanthanum manganite (LSM) electrodes, the latter being an electronically conducting metal oxide, was investigated in laboratory and engine testing. Preliminary results indicated that gold electrodes have good stability and the potential for low water cross-sensitivity, but also have a higher thermal expansion coefficient and lower melting temperature than the YSZ electrolyte, which limit processing flexibility. LSM electrodes have high melting temperatures and better thermal expansion match with YSZ, but have shown higher water cross-sensitivity than gold.

Experimental

Two different sensing materials, Au and LSM, were investigated. Figure 2a shows a schematic of a prototype using Au wire as the sensing electrode and alumina with an imbedded Pt resistive heater as the substrate (70 mm × 4 mm × 1 mm, see Fig. 1a). The substrate has a total of four leads, two leads for the Pt resistive heater located on one side, and two leads for the sensor located on the opposite side.

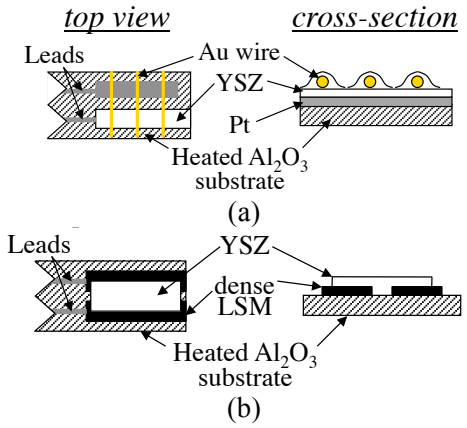

Figure 2. Schematic of NO_x prototype sensors using either (a) Au wire or (b) dense LSM as the sensing electrode.

One of the substrate leads contacted the Pt counter electrode. Yttria-stabilized zirconia (YSZ, 8 mol% yttria doping) slurry was then applied on top of the Pt. Au wires were then added and additional YSZ slurry was applied on top of the wires with the entire assembly fired at 1000°C to produce the porous YSZ electrolyte. The second substrate lead for the sensor housing contacted the Au wire.

Figure 2b shows a schematic of the prototype using LSM as the sensing electrode. A dense pellet was prepared with commercial $(La_{0.85}Sr_{0.15})_{0.98}Mn$ oxide powder (Praxair) by pressing in a uniaxial die and sintering at 1250°C. Two pieces of LSM (6 mm × 2 mm × 1 mm) were machined and attached to the top of the substrate using Pt paste and fired to 1200°C. YSZ slurry was applied on top of the dense LSM pieces and the assembly fired at 1000°C.

A laboratory study of both the Au wire and LSM prototypes was also performed using 0.5 mm thick alumina substrates without imbedded heaters to evaluate aging and reproducibility. The alternative substrate was more suitable for longer-term continuous controlled temperature testing in a laboratory tube furnace. The sensor geometries were similar to that shown in Fig. 2.

LSM prototypes were found to have more variability in aging and reproducibility, so a subset of laboratory experiments focused on evaluating only LSM prototypes using modified substrate compositions. The modified substrate compositions were used to investigate the role of thermal expansion mismatch between the sensor components and the underlying substrate. Modified substrate compositions included YSZ substrates with thermal expansion behavior to match the prototype sensor YSZ electrolyte. YSZ substrates coated with a thin alumina layer were also used to identify the role of electrical insulation between sensor components and the underlying substrate while still maintaining better thermal expansion match.

YSZ substrates were prepared with commercial powders pressed into dense pellets using a uniaxial die before firing at 1500°C. Alumina-coated YSZ substrates were prepared with a thin alumina layer applied using a slurry painted onto the unfired dense pellet before co-firing at 1500°C.

Laboratory experiments were performed in a quartz tube (21.4 mm I.D.) placed inside a tube furnace with both electrodes exposed to the same environment. The gas composition was controlled by mixing air, N_2, and a 1000 ppm NO/NO_2 feed using a standard gas handling system equipped with thermal mass flow controllers. The total gas flow rate was fixed at 1000 ml/min. Measurements were made at 650°C.

For the subset of experiments focused on evaluating LSM prototypes using modified substrate compositions, prior to testing, sensors were 'burned-in' for a period of 68 ± 5 hours at 650°C in 10.5% O_2. During this time, impedance and phase angle were measured using a constant frequency 5 Hz, 100 mV signal. Testing began immediately following this burn-in procedure. To test sensors, impedance measurements were performed at 550, 600, and 650°C in 10.5% O_2 with varying levels of added NO. Impedance phase angle (θ_{5Hz}) was used to measure sensor response to step changes in NO content. The step changes followed the protocol 0, 100, 80, 60, 50, 40, 30, 20, 15, 10, 5, and back to 0 ppm with 2 minutes between the steps. For analysis of the sensor response to different NO concentrations, signals were averaged over one minute of data collection, approximately 30 seconds prior to and 30 seconds after each step change.

Dynamometer engine testing of real diesel exhaust was performed at Ford Research Center using an engine test cell fitted with engine gas recirculation (EGR) and a urea-based selective catalytic reduction (SCR) system for reducing NO_x emissions. The exhaust gas composition was evaluated with a chemiluminescent NO_x analyzer and a paramagnetic oxygen analyzer. Prototype sensors were packaged with a housing (see Fig. 1b) and directly mounted into the exhaust tailpipe manifold alongside a commercially available NO_x sensor.

For laboratory testing, impedance measurements were performed using a Solartron 1260 Impedance Analyzer in combination with a Solartron 1287 Electrochemical Interface. Dynamometer engine testing at Ford used a stand-alone Solartron 1260 Impedance Analyzer. Computer-controlled data acquisition used the commercially available ZPlot software (Scribner Associates, Inc.).

Results and Discussion

Laboratory testing: Longer-term aging studies of Au and LSM

A laboratory study of both the Au wire and LSM prototypes was performed using 0.5 mm thick alumina substrates without imbedded heaters to evaluate aging and reproducibility. Previous testing had indicated stable response for older generation prototypes (prior to FY2012) using either Au or LSM at aging times of up to 500 hrs. Continued testing of more recent FY 2012 prototypes with newer YSZ slurry formulations confirmed the stability of Au-based prototype sensors, but indicated some variation among samples in LSM performance, including some with signal drift.

Figures 3 and 4 show results for the two prototype sensors (Au and LSM) tested side-by-side for measurements at 5 Hz and 100 mV excitation, where the left y-axis corresponds to the phase angle signal of the Au prototype sensor while the right y-axis corresponds to the LSM prototype sensor signal. In Fig. 3, the dynamic prototype sensor response is shown in 10.5% O_2 when 100 ppm of NO is introduced, with time on the x-axis in minutes. The Au prototype sensor showed identical dynamic response when testing at 24 hrs, at ~500hrs, and again at nearly 1000 hrs. The LSM prototype sensor, however, showed baseline drift at those same aging times, although maintaining overall sensitivity to 100 ppm NO.

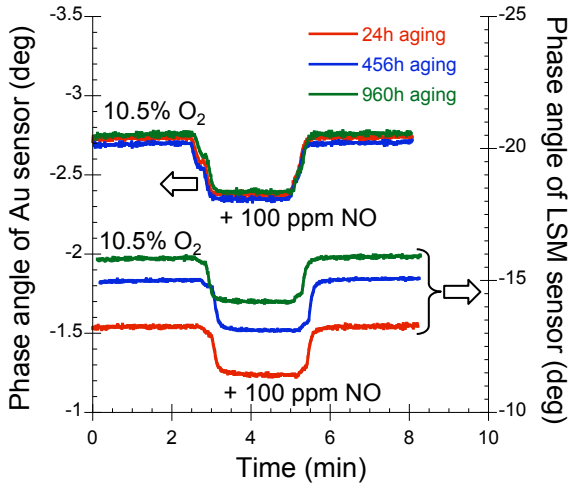

Figure 3. Phase angle response of Au prototype (left y-axis) and LSM prototype (right y-axis) in 10.5% O_2 with 2 min addition of 100 ppm NO at different aging times.

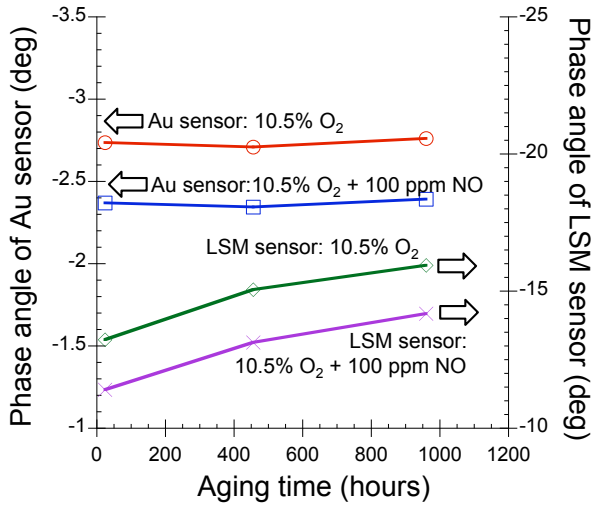

Figure 4. Plot of phase angle response of Au prototype (left y-axis) and LSM prototype (right y-axis) vs. aging time that corresponds to data in Fig. 3 for 10.5% O_2 with and without addition of 100 ppm NO.

In Fig. 4, the prototype sensor signal (i.e., phase angle) is shown for different aging times for Au (left y-axis) and LSM (right y-axis), with aging time in hours on the x-axis. The poor sample-to-sample reproducibility of LSM prototype sensors and variability in performance was attributed to the formation and growth of random microcracks due to thermal expansion mismatch between the sensor components (YSZ and LSM) and the substrate (alumina). The micro-cracks were observed on some sensors after processing at 1000°C. Figure 5 shows a micrograph of a typical microcrack that was visible within the lower strength porous YSZ electrolyte after processing. Cracks up to ~30 μm thick have been observed, while some sensors showed no visible cracking. However, alumina is an ideal substrate material because of its high electrical resistivity, inertness, and proven compatibility with embedded heaters. In addition, while micro-cracking was sporadically observed in the sensors evaluated here, it is believed that this issue will be resolved with design modification and improved mass manufacturing processes.

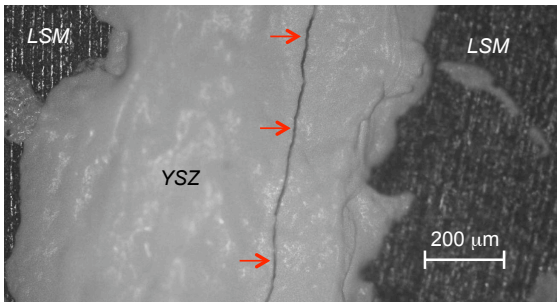

Figure 5. Example of visible micro-cracking occurring on the top surface of the porous YSZ electrolyte.

Laboratory testing: Modifying substrate composition to improve LSM prototypes

To provide guidance in mitigating micro-cracking in the LSM prototype sensors, a subset of laboratory experiments examined the effect of different substrate compositions with different thermal expansions. Table 1 shows the thermal mismatch between the materials used in the LSM prototype sensor discussed above (see Fig. 2b).

Table 1. Coefficients of thermal expansion for materials used in LSM prototype sensors.

Material	Coefficient of thermal expansion (10^{-6}/°C)
Al_2O_3	8
YSZ	10.5
LSM	10

Dense YSZ substrates were used because they have identical thermal expansion match to the porous YSZ electrolyte. YSZ substrates with thin Al_2O_3 coating layers were also fabricated to increase electrical resistance of substrates without signifi-

cantly altering their thermal expansion mismatch with the porous YSZ electrolyte. For sensors using both of these substrate types, there was no visible microcracking in the top surfaces of the YSZ electrolyte layers. It has not yet been confirmed that cracks do not exist subsurface of the YSZ electrolyte, although this is not thought to be likely.

The effects of microcracking on impedancemetric sensor performance were evaluated using the phase angle response at 5 Hz, labeled as θ_{5Hz}. Higher θ_{5Hz} magnitude is generally desirable to improve signal resolution. The baseline (0 ppm NO_x) θ_{5Hz} magnitude signal was determined by averaging steady-state data points taken every 20 seconds for two hours during the burn-in procedure between 60 and 62 hrs. Figure 6 shows results comparing the baseline values for the three different substrates, as well as sensor-to-sensor reproducibility.

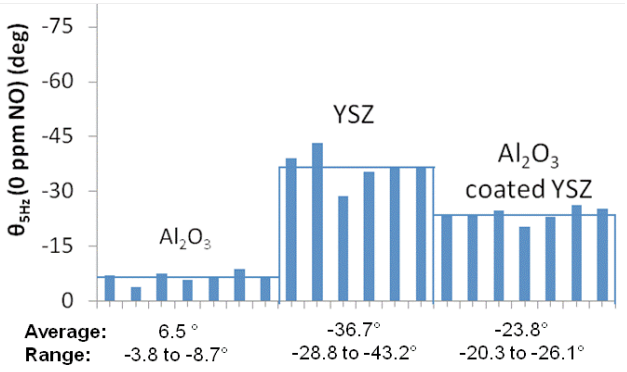

Figure 6. Baseline (0 ppm NO) values for 5 Hz phase angles at 650°C in a 10.5% O_2 for replicate sensors built on Al_2O_3, YSZ, or Al_2O_3 coated YSZ substrates; average of each substrate group is also shown.

Baseline values were consistently highest for sensors on YSZ substrates, followed by sensors on Al_2O_3 coated YSZ substrates, and then sensors on Al_2O_3 substrates. Al_2O_3 coated YSZ substrates gave the best sensor-to-sensor reproducibility of baseline values. Sensor response to varying concentrations of NO is shown in Figure 7. All sensors in this study had rapid responses, with response times (10-90%) of approximately 5 seconds.

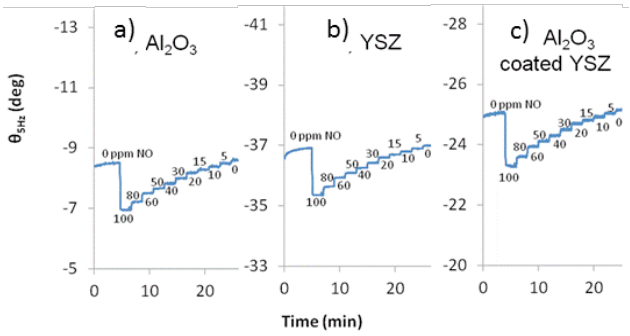

Figure 7. Sensor response as measured using the phase angle at 5 Hz phase (θ_{5Hz}) for sensors built on (a) Al_2O_3, (b) YSZ, and (c) Al_2O_3 coated YSZ at 650°C in a 10.5% O_2.

Irrespective of substrate, all sensors showed high sensitivity to NO. In addition, a linear dependence on NO concentration in the range of 0-20 ppm was observed for sensors built on all three substrates, as shown in Figure 8. Sensitivity declined at higher NO concentrations, which is in line with our previous results.[11]

Linear fits to the data in the 0-20 ppm NO range determined that the sensitivity to NO_x was relatively independent of substrate and temperature at the three temperatures employed (550, 600, and 650 °C). The average NO sensitivity for the six replicate sensors was 0.019, 0.017, and 0.016 deg/ppm for sensors on YSZ, Al_2O_3 coated YSZ, Al_2O_3 substrates, respectively. This indicates that microcracking, apparent on the Al_2O_3 substrates in particular, had minimal influence on sensitivity to NO. If microcracking should cease after a given time period, the sensors may remain functional. However, degradation in sensor performance, and ultimate failure would be anticipated if the cracking continued to longer time scales.

Future designs using Al_2O_3 substrates will need to address the thermal mismatch between Al_2O_3 and YSZ to avoid microcracking in the YSZ electrolyte. One approach could be to use alternative designs with the electrode-electrolyte interfaces in the same plane as the substrate. Another approach could be to reduce the occurrence rate of microcracking by altering the high temperature processing procedure. Such alterations may include reducing the heating/cooling rates, dwelling at intermediate temperatures, or reducing the final processing temperature.

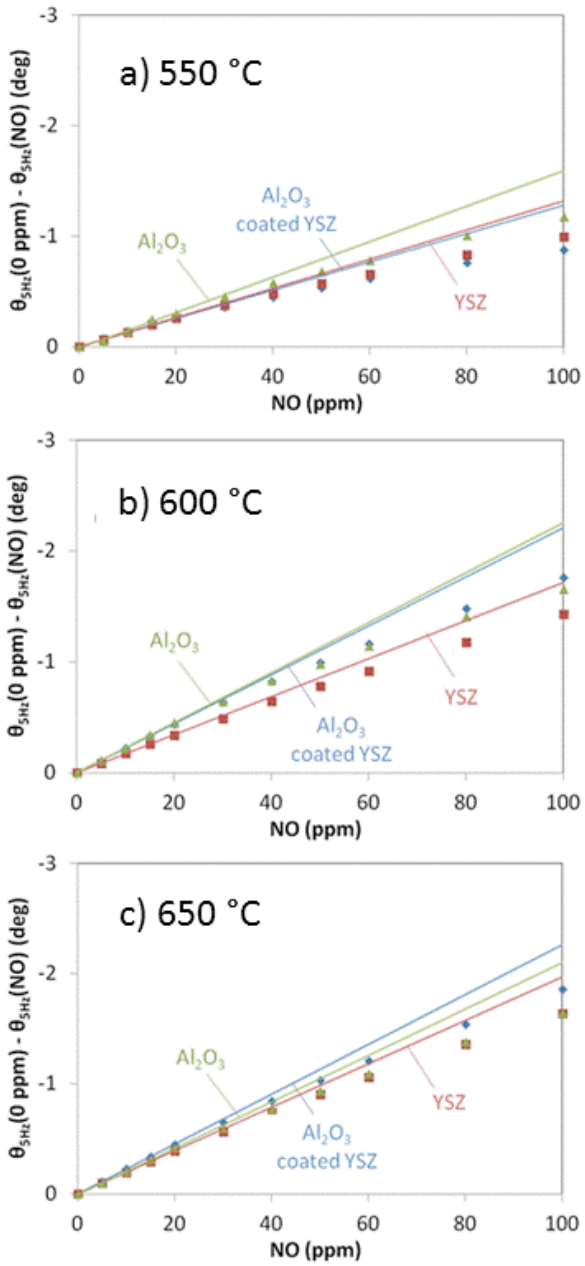

Figure 8. Average sensor response as measured by θ_{5Hz} for sensors built on Al_2O_3 (green triangles), YSZ (red squares), or Al_2O_3 coated YSZ (blue diamonds) substrates at (a) 550, (b) 600, and (c) 650°C. Linear fits to data for 0-20 ppm NO are also shown.

Dynamometer engine testing of FY2012 prototypes

Dynamic dynamometer engine testing of FY2012 prototypes was conducted at Ford Research Center. Prototype sensors were packaged by a U.S. supplier into appropriate housings (see Fig. 1b) and then placed directly in the exhaust manifold at the tailpipe for exposure to real-world diesel exhaust. Figure 9 shows dynamic data from a portion of EPA US06 or Supplemental Federal Test Procedure (SFTP), which is a high acceleration aggressive dynamometer driving schedule; time, in seconds, is on the x-axis.

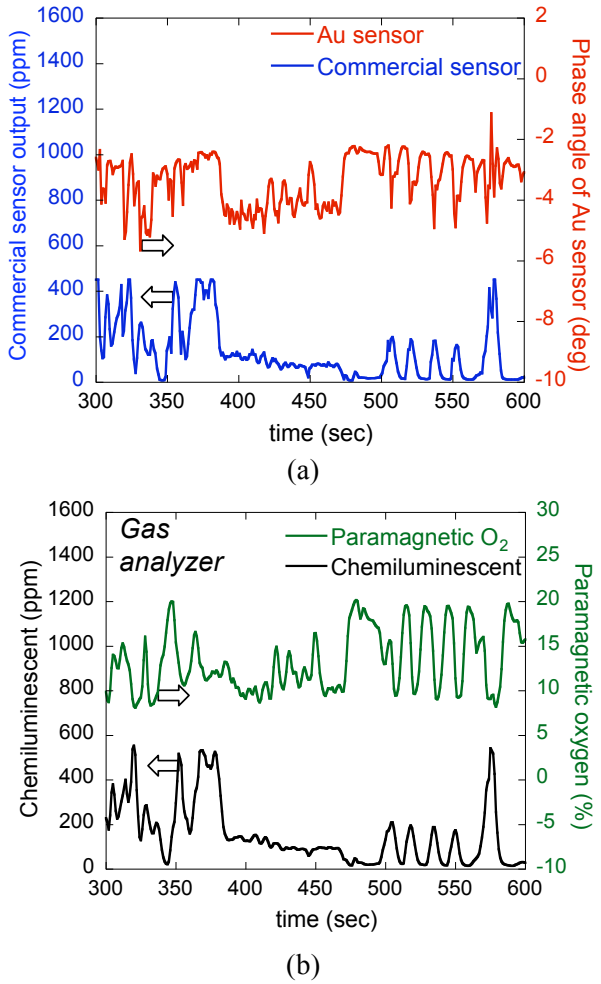

Figure 9. Dynamometer test: (a) Phase angle response of Au prototype sensor (red, right y-axis) compared with a commercial NO_x sensor (blue, left y-axis) and (b) data from paramagnetic oxygen analyzer (green, right y-axis) and chemiluminescent NOx analyzer (black, left y-axis).

In Fig. 9a, the left y-axis corresponds to the commercial sensor output (blue curve) and the right y-axis corresponds to the raw phase angle output from the Au prototype sensor (red curve), showing reasonable agreement. In Fig. 9b, data taken simultaneously using bench analyzers are shown, where the left y-axis corresponds to the chemiluminescent analyzer (black curve) and the right y-axis corresponds to the paramagnetic oxygen analyzer (green curve). As expected, the oxygen response from about 425 to 450 sec. is seen in both the Au proto-

type sensor (Fig. 9a, red curve, right y-axis) and in the paramagnetic oxygen analyzer (Fig. 9b, green curve, right y-axis).

Commercial sensors include data processing and electronics whereas the measurement with the Au prototype sensor only included the raw phase angle signal without any additional processing. During actual advanced operation of the prototype sensor, additional signal processing will be necessary to remove oxygen interference. Previously, we have demonstrated algorithms suitable for compensating for interferences.[12] Future work includes working with our CRADA partners (EmiSense) to design appropriate electronics and refine strategies for reducing interferences when the NO_x sensors are used in OBD II systems.

Additional FY2012 testing at Ford Research Center included evaluation on an advanced high-flow (40 Liters/min) test stand with controlled mass flow controllers to alter a range of gas concentrations (O_2, CO_2, H_2O, and NO_x). The test stand also included output from a commercial sensor located near the prototype sensor under evaluation. These data are now being used to further refine strategies for reducing interferences.

Other research highlights in FY2012

To further understand impedancemetric sensing mechanisms and to guide improvement of materials and geometries for mass manufacturing and commercialization, alternative configurations of the LSM prototype sensor were investigated. An asymmetric (LSM/YSZ/Pt) through-plane geometry, shown in Fig. 10, was evaluated that differs from the previously discussed symmetric (LSM/YSZ/LSM) in-plane configuration (see Fig. 2b). As previously discussed, the electrode-electrolyte interfaces in the same plane as the substrate could reduce microcracking.

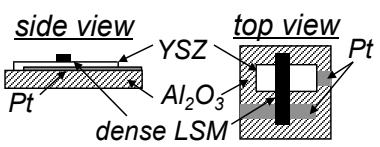

Figure 10. Schematic of alternative asymmetric NO_x prototype sensor using dense LSM as the sensing electrode.

Preliminary results indicated that the alternative through-plane geometry seemed to inhibit crack growth within the YSZ electrolyte leading to more reproducible behavior. Also, the through-plane geometry with a thin YSZ electrolyte layer (~100-250 μm) should lead to improved ionic conductivity and reduced bulk ionic resistance, which may also improve performance. The alternative asymmetric LSM prototype sensor geometry also provides a platform for elucidating the contributions from the Pt and LSM electrodes as well as the YSZ electrolyte resistance to the overall sensing performance. Electrochemical evaluation and sensor performance testing is ongoing and continues into FY2013. A more complete analysis of data obtained using the three different sensor prototypes will be provided in an upcoming publication.

Conclusions

Work in FY2012 continued to build on previous efforts to modify prototypes to improve performance. Although previous aging studies indicated good long-term performance of both Au and LSM prototype sensors, more recent laboratory testing indicated variability (sample-to-sample reproducibility) in drift behavior for the LSM prototype sensors. Altering substrate composition to reduce thermally induced strain and the subsequent formation of microcracks improved sensor performance, and would be a viable option for resolving the issue during mass manufacturing.

Engine dynamometer testing of FY2012 prototype sensors at Ford Research Center confirmed robustness and durability seen in previous testing. The prototype sensor showed reasonable agreement with a commercially available sensor. Additional electronics and strategies are being developed with our CRADA partners to reduce interferences.

Other progress in FY2012 included alternative geometries for the LSM prototype sensor to improve performance. An asymmetric through-plane geometry was investigated with preliminary results indicating improved sample-to-sample reproducibility. The alternative geometry also serves as a platform for elucidating the contributions from the Pt and LSM electrodes as well as the YSZ electrolyte resistance to the overall sensing performance. Electrochemical evaluation and sensor performance testing is ongoing and continues into FY2013.

A major milestone for this past year was the development of a CRADA with EmiSense Technologies, who have licensed the LLNL NO_x sensor technology. EmiSense has extensive experience and resources for the development of emission control

sensors, and the partnership with EmiSense will accelerate efforts to bring the LLNL NO_x sensor technology to commercialization. We continue our long-standing collaboration with Ford Motor Company in this effort.

References

1. N. Yamazoe, *Sens. Actuators, B*, **108**, 2 (2005).
2. R. Moos, *Int. J. Appl. Ceram. Technol.*, **2**, 401 (2005).
3. S. Akbar, P. Dutta, and C. Lee, *Int. J. Appl. Ceram. Technol.*, **3**, 302 (2006).
4. F. Menil, V. Coillard, and C. Lucat, *Sensors and Actuators B,* **67**, 1 (2000).
5. S. Zhuiykov and N. Miura, *Sens. Actuators, B*, **121**, 639 (2007).
6. J. W. Fergus, *Sens. Actuators, B*, **121**, 652 (2007).
7. S. -W. Song, L. P. Martin, R. S. Glass, E. P. Murray, J. H. Visser, R. E. Soltis, R. F. Novak, and D. J. Kubinski, *J. Electrochem. Soc.*, **153**, H171 (2006).
8. L. P. Martin, L. Y. Woo, and R. S. Glass, *J. Electrochem. Soc.,* **154**, J97 (2007).
9. L. Y. Woo, L. P. Martin, R. S. Glass, and R. J. Gorte *J. Electrochem. Soc.,* **154**, J129 (2007).
10. L. Y. Woo, L. P. Martin, R. S. Glass, W. Wang, S. Jung, R. J. Gorte, E. P. Murray, R. F. Novak, and J. H. Visser. *J. Electrochem. Soc.,* **155**, J32 (2008).
11. L.Y. Woo, R.S. Glass, R.F. Novak, and J.H. Visser. *J. Electrochem. Soc.*, **157**, J81 (2010).
12. L.Y. Woo, R.S. Glass, R.F. Novak, and J.H. Visser. *Sensor Actuat. B-Chem.*, **157**, 115 (2011).

Publications/Presentations

W. L. Du Frane, L.Y. Woo, R.S. Glass, R.F. Novak, and J.H. Visser, "Substrate Effects on Electrochemical NO_x Sensor Based on Porous Y_2O_3-Stabilized ZrO_2 (YSZ) and Sr-doped $LaMnO_3$ (LSM), presented at the 221st Meeting of the Electrochemical Society, in Seattle, Washington May 6-10, 2012.

W. L. Du Frane, L.Y. Woo, R.S. Glass, R.F. Novak, and J.H. Visser, "Substrate Effects on Electrochemical NO_x Sensor Based on Porous Y_2O_3-Stabilized ZrO_2 (YSZ) and Sr-doped $LaMnO_3$ (LSM). *ECS Transactions*, submitted 2012.

L.Y.Woo and R. S. Glass, "NO_x Sensor Development," project ID #PM005, Annual Merit Review and Peer Evaluation. Washington, D.C., May 15, 2012.